Intelligent Adaptation Mechanism of Full-Order Luenberger Observer based on Fuzzy Logic Applied to Direct Control by Flux Orientation without Speed Sensor for Doubly Fed Induction Motor

DJAMILA CHERIFI, YAHIA MILOUD
Department of Electrical Engineering,
University of Dr.Tahar Moulay,
Saida GACA Laboratory,
ALGERIA

Abstract: - The present work focused on the control by flow orientation without mechanical sensors on the doubly fed induction motor by the use of artificial intelligence techniques. Our main contribution lies in the development of control methodologies to improve control by flux orientation, for this, we acted on the type and control of inverters by the use of multilevel inverters and then on the observation technique of rotor speed based on the high gain Luenberger observer and improvements to the speed adaptation mechanism using fuzzy logic. Simulation tests of the proposed improvement approach were carried out at the end of this work to verify the behavior of this system in the face of different types of training.

Key-Words: - artificial intelligences, doubly fed induction motor, field-oriented control, fuzzy logic, multi-level inverter, Luenberger observer.

Received: February 29, 2023. Revised: December 19, 2023. Accepted: February 23, 2024. Published: April 9, 2024.

1 Introduction

The three-phase asynchronous machine powered by a voltage inverter is a drive system with many advantages: a simple, robust, and inexpensive machine structure, and control techniques that have become efficient thanks to advances in semiconductors. Power and digital technologies. This converter-machine assembly, however, remains restricted to the lower limit of the high power range (up to a few MW), due to the electrical constraints experienced by the semiconductors and their low switching frequency, [1], [2], [3], [4]. In the field of high-power drives, other solutions are using the reciprocating machine operating in a somewhat particular mode, these are double-fed induction machines "DFIM": are three-phase asynchronous machines with a wound rotor, which can be powered by two voltage sources, one of the stator and the other at the rotor, [5], [6].

Despite all these qualities mentioned above, many problems remain. Its control, on the other hand, that of the direct current machine, [7], is more difficult given the non-linearity and the strong coupling of its model due to the absence of natural decoupling between the different input-output variables, [8]. Considerable progress, both in the fields of power electronics and micro-electronics, has made it possible to implement adequate controls for this machine, making it a machine that guarantees performances similar to those obtained by the control of a DC machine with separate excitation. Along with these technological advances, the scientific community has developed numerous control strategies in the literature, the most popular of which is vector control in its different versions to control the flux and torque of the asynchronous machine in real-time, [9], [10], [11].

Whether it is these commands, the control of the speed and the position of the rotor requires the presence of an incremental encoder (a sensor). However, this sensor must be placed in its environment of use and provide additional space for its installation. Something which leads to an increase in cost and a weakening of the drive system. In addition, the introduction of this fragile device leads to a reduction in the reliability of the system which requires special care for itself. Something that is not always desirable or possible, [12], [13].

For reasons of reliability and economy, the idea of replacing the mechanical sensor with another of the algorithm type was born and control without a speed sensor has become a serious subject of study for research in recent years. It is then necessary to have record estimation or observation techniques to reconstruct the speed and position of the rotor from the information collected by measuring the electrical terminals of the machine's stator. It is therefore important, when developing the control without a speed sensor, to emphasize dynamic (pursuit) and static (rejection) performance, [14], [15].

Currently, the study of DFIM powered by static converters constitutes a vast research theme in electrical engineering laboratories. This research work has led to the appearance of new power converter structures intended for high-voltage applications called multilevel converters. The use of multilevel converters in high power and high voltage areas makes it possible to simultaneously resolve the difficulties relating to the size and control of groups of two-level inverters generally used in this type of application. To satisfy certain optimization criteria, namely the reduction of harmonics, [16], [17]. Improving these classic techniques is the concern of several researchers. This improvement consists of a compromise between performance and robustness on the one hand, and simplicity and cost on the other hand. Thus, intelligent controls that have appeared in recent years, making it possible to reproduce human reasoning and which are based on fuzzy logic, currently occupy an important place in the field of machine controls, [18], [19].

Our work consists of proposing contributions to improving the performance and robustness of the sensorless control of the DFIM by integrating the concept of fuzzy logic into the speed adaptation mechanism of the Luenberger observer.

The present work devoted to the implementation of an algorithm for observing the speed of a DFIM powered by two five-level inverters using the high-gain Luenberger observer based on fuzzy logic. At the end of the work, we will present simulation results to show the performance of this approach.

2 System Modeling

2.1 Mathematical Modeling of DFIM

For the double-fed induction machine, the control variables are the stator and rotor voltages. Considering the stator currents and the rotor fluxes as state variables, then the DFIM model is described by the following equation, [20]:

$$\begin{cases} \frac{d}{dt}i_{sd} = -\lambda i_{sd} + \omega_s i_{sq} + \frac{K}{T_r}\phi_{rd} + \omega.K\phi_{rq} + \frac{1}{\sigma L_s}v_{sd} + K\,v_{sd} \\ \frac{d}{dt}i_{sq} = -\omega_s i_{sq} - \lambda i_{sq} - \omega.K\phi_{rd} + \frac{K}{T_r}\phi_{rq} + \frac{1}{\sigma L_s}v_{sq} + K\,v_{sq} \\ \frac{d}{dt}\phi_{rd} = \frac{L_m}{T_r}i_{sd} - \frac{1}{T_r}\phi_{rd} + \omega.\phi_{qr} + v_{rd} \\ \frac{d}{dt}\phi_{rq} = \frac{L_m}{T_r}i_{sq} - \omega.\phi_{rd} - \frac{1}{T_r}\phi_{rq} + v_{rq} \\ \frac{d}{dt}\omega = p^2\frac{L_m}{L_r}(\phi_{rd}i_{sq} - \phi_{rq}i_{sd}) - \frac{f}{J}\omega - \frac{C_r}{J} \end{cases} \tag{1}$$

with

$$T_r = \frac{L_r}{R_r};\ T_s = \frac{L_s}{R_s};\ \lambda = \frac{1}{\sigma.T_r};\ K = \frac{L_m}{\sigma L_s.L_r};\ \sigma = 1 - \frac{L_m^2}{L_s L_r}$$

2.2 Model of a Five-Level Inverter Type NPC

The configuration of a five-level NPC-type inverter is illustrated in Figure 1, for this type of assembly we use four pairs of complementary transistors each one with an antiparallel diode, the number of locking diodes is six, and four capacitors allow the input voltage to be divided into four equal voltages, it should be noted that each main switch is sized to block a voltage level (E/4), [21], [22], [23]:

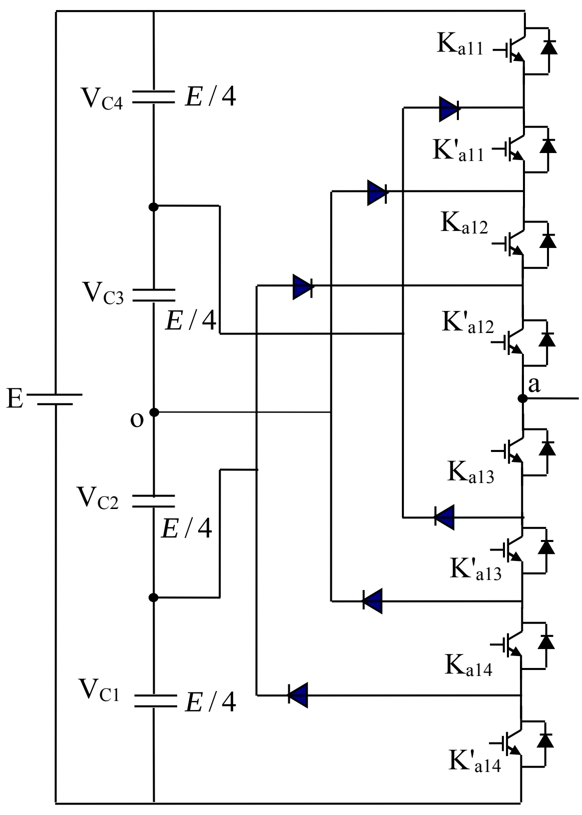

Fig. 1: Structure of a phase of a five-level NPC inverter

2.3 Switching Functions

For each switch K_{xi} (i= 11… 14, x= a, b and c), we define a switching function as follows:

$$F_{xi} = \begin{cases} 1 & if \quad K_{xi} \quad is \text{ closed} \\ 0 & if \quad K_{xi} \quad is\ open \end{cases}$$

The switch controls for the lower half-arms are complementary to those for the upper half-arms:

$$F_{xi} = 1 - F_{x(i-4)}$$

2.4 Principle of Operation of a Five-Level NPC Inverter

For this type of inverter, there are only five functional sequences:

- Vao = +E/2 ⇒[1 1 1 1 0 0 0 0]: switches k_{11} k'_{11} k_{12} k'_{12} are ordered at closing, tends that k_{13} k'_{13} k_{14} k'_{14} are ordered at the opening

- Vao = +E/4 ⇒[0 1 1 1 1 0 0 0]: switches k'_{11} k_{12} k'_{12} k_{13} are ordered at closing, tends that k'_{13} k_{14} k'_{14} k_{11} are ordered at the opening.

- Vao = 0 ⇒[0 0 1 1 1 1 0 0]: the switches k_{12} k'_{12} k_{13} k'_{13} are ordered at closing, tends that k_{14} k'_{14} k_{11} k'_{11} are ordered at the opening.

- Vao = −E/4 ⇒[0 0 0 1 1 1 1 0]: the switches k'_{12} k_{13} k'_{13} k_{14} are ordered at closing, tends that k'_{14} k_{11} k'_{11} k_{12} are ordered at the opening.
-
- Vao = −E/2 ⇒[0 0 0 0 1 1 1 1]: the switches k_{11} k'_{11} k_{12} k'_{12} are ordered at opening, so that k_{13} k'_{13} k_{14} k'_{14} are ordered at closing.

The vector control of the DFIM requires the installation of an incremental encoder to be able to measure the rotor speed or position. The disadvantages inherent in the use of this mechanical sensor, placed on the machine shaft, are multiple. First, the presence of the sensor increases the volume and overall cost of the system. Then, it requires an available piece of shaft, which can constitute a disadvantage for small machines. Finally, the reliability of the system decreases because of this fragile device which requires special care for itself. Under these conditions, it is necessary to reconstruct the state of the machine from easily measurable or estimable stator voltages and currents. Several strategies have been proposed in the literature to achieve this goal. The proposed methods are based on estimators and observers which lead to the implementation of simple and fast algorithms depending on the model of the asynchronous machine, [24]. This work proposes a Luenberger observer-type observation technique for rotor speed and flux for DFIM without a mechanical sensor.

3 Principle of an Observer

The structure of a state observer is shown in Figure 2. It firstly involves an estimator operating in an open loop which is characterized by the same dynamics as that of the system. The structure operating in a closed loop obtained by the introduction of a gain matrix "L" makes it possible to impose the dynamics specific to this observer, [25].

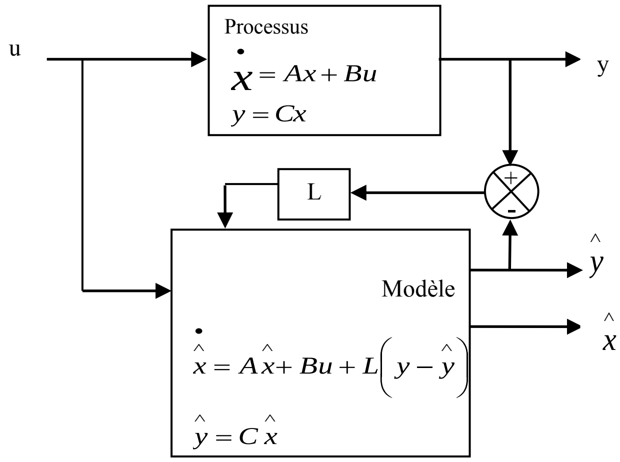

Fig. 2: Principle of a state observer

This observer principle diagram (Figure 2) makes it possible to use all kinds of observers, their difference being located only in the synthesis of the gain matrix "L".

3.1 Determination of the Gain Matrix L

The determination of the "L" matrix uses the conventional pole placement procedure. We proceed by imposing the poles of the observer and consequently its dynamics. We determine the coefficients of "L" by comparing the characteristic equation of the observer "$\det(\lambda I - (A - LC)) = 0$" with the one we wish to impose, [26], [27].

The machine model equations are expressed by:

$$\begin{cases} \dot{x} = Ax(t) + Bu(t) \\ y(t) = Cx(t) \end{cases} \tag{2}$$

The state model of the Luenberger observer used for the estimation of the rotor flux and the (measured) stator currents is given by:

$$\begin{cases} \dot{\hat{x}} = A\hat{x}(t) + Bu(t) + L(y(t) - \hat{y}(t)) \\ \hat{y}(t) = C\hat{x}(t) \end{cases} \tag{3}$$

Or in the form

$$\begin{cases} \dot{\hat{x}} = (A - LC)\hat{x}(t) + Bu(t) + Ly(t) \\ \hat{y}(t) = C\hat{x}(t) \end{cases} \tag{4}$$

with

$x = \begin{bmatrix} i_{sd} & i_{sq} & \phi_{rd} & \phi_{rq} \end{bmatrix}^T$; $\hat{x} = \begin{bmatrix} \hat{i}_{sd} & \hat{i}_{sq} & \hat{\phi}_{rd} & \hat{\phi}_{rq} \end{bmatrix}^T$; $y = \begin{bmatrix} i_{sd} & i_{sq} \end{bmatrix}^T$; $u = \begin{bmatrix} v_{sd} & v_{sq} & v_{rd} & v_{rq} \end{bmatrix}^T$

The estimation error is determined by the difference:

$$\dot{e}(t) = (A - LC)e(t) \tag{5}$$

This error will converge towards zero by a suitable choice of the gain matrix "L" to make the matrix $A_0 = (A - LC)$ stable, or the eigenvalues of this matrix are negative real parts. The method of imposing the poles consists of choosing the poles of the observer to accelerate its dynamics about the system (the poles of the observer are proportional to those of the motor),

Let's define the matrix "L" in its specific form:

$$L = \begin{bmatrix} L_1 I + L_2 J \\ L_3 I + L_4 J \end{bmatrix}^T \tag{6}$$

L_1, L_2, L_3, L_4 sont données par :

$$\begin{cases} L_1 = (k-1)\left(\gamma + \dfrac{1}{T_r}\right) \\ L_2 = (k-1).\hat{\omega}_r \\ L_3 = \dfrac{(k^2-1)}{\delta}\left(\gamma - \delta \dfrac{L_m}{T_r}\right) + \dfrac{(k-1)}{\delta}\left(\gamma + \dfrac{1}{T_r}\right) \\ L_4 = \dfrac{(k-1)}{\delta}\hat{\omega}_r \end{cases} \tag{7}$$

Or k : Positive constant

The poles of the observer are chosen to accelerate its convergence about the dynamics of the open loop system in general, but they must remain slow about the measurement noise, which means that we choose the constant k usually small.

4 Application of the Luenberger Observer to the DFIM

4.1 State Model of the DFIM in the Reference (α,β)

The DFIM model in the reference (α,β) is defined by the following system of equations :

$$\begin{cases} \dot{i}_{s\alpha} = -\lambda i_{s\alpha} + \omega_s i_{s\beta} + \dfrac{K}{T_r}\phi_{r\alpha} + \omega.K\phi_{r\beta} + \dfrac{1}{\sigma L_s}v_{s\alpha} + K v_{s\alpha} \\ \dot{i}_{s\beta} = -\omega_s i_{s\alpha} - \lambda i_{s\beta} - \omega.K\phi_{r\alpha} + \dfrac{K}{T_r}\phi_{r\beta} + \dfrac{1}{\sigma L_s}v_{s\beta} + K v_{s\beta} \\ \dot{\phi}_{r\alpha} = \dfrac{L_m}{T_r}i_{s\alpha} - \dfrac{1}{T_r}\phi_{r\alpha} + \omega.\phi_{r\beta} + v_{r\alpha} \\ \dot{\phi}_{r\beta} = \dfrac{L_m}{T_r}i_{s\beta} - \omega.\phi_{r\alpha} - \dfrac{1}{T_r}\phi_{r\beta} + v_{r\beta} \end{cases} \tag{8}$$

with: $\mathrm{Tr} = \dfrac{L_r}{R_r}$; $T_s = \dfrac{L_s}{R_s}$; $\lambda = \dfrac{1}{\sigma.T_r}$; $K = \dfrac{L_m}{\sigma L_s.L_r}$

4.2 State Representation of the Luenberger Observer

As the state is generally not accessible, the objective of an observer consists of carrying out a command by feedback of the state and estimating this state of a variable which we will note $\hat{X}$

Such as : $\hat{X} = [\hat{i}_{s\alpha} \quad \hat{i}_{s\beta} \quad \hat{\phi}_{r\alpha} \quad \hat{\phi}_{r\beta}]^T$

According to equation (2), we can represent the observer by the following system of equations:

$$\begin{cases} \dot{\hat{i}}_{s\alpha} = -\lambda\hat{i}_{s\alpha} + \omega_s\hat{i}_{s\beta} + \dfrac{K}{T_r}\hat{\phi}_{r\alpha} + \omega.K\hat{\phi}_{r\beta} + \left(\dfrac{1}{\sigma L_s}\right)V_{s\alpha} + KV_{r\alpha} + L_1\left(i_{s\alpha} - \hat{i}_{s\alpha}\right) - L_2\left(i_{s\beta} - \hat{i}_{s\beta}\right) \\ \dot{\hat{i}}_{s\beta} = -\omega_s\hat{i}_{s\alpha} - \lambda\hat{i}_{s\beta} - \omega.K\hat{\phi}_{r\alpha} + \dfrac{K}{T_r}\hat{\phi}_{r\beta} + \left(\dfrac{1}{\sigma L_s}\right)V_{s\beta} + KV_{r\beta} + L_2\left(i_{s\alpha} - \hat{i}_{s\alpha}\right) - L_1\left(i_{s\beta} - \hat{i}_{s\beta}\right) \\ \dot{\hat{\phi}}_{r\alpha} = \dfrac{L_m}{T_r}\hat{i}_{s\alpha} - \dfrac{1}{T_r}\hat{\phi}_{r\alpha} + \omega.\hat{\phi}_{r\beta} + V_{r\alpha} + L_3\left(i_{s\alpha} - \hat{i}_{s\alpha}\right) - L_4\left(i_{s\beta} - \hat{i}_{s\beta}\right) \\ \dot{\hat{\phi}}_{r\beta} = \dfrac{L_m}{T_r}\hat{i}_{s\beta} - \omega.\hat{\phi}_{r\alpha} + \dfrac{1}{T_r}\hat{\phi}_{r\beta} + V_{r\beta} + L_4\left(i_{s\alpha} - \hat{i}_{s\alpha}\right) - L_3\left(i_{s\beta} - \hat{i}_{s\beta}\right) \end{cases} \tag{9}$$

This leads to the equation:

$$\begin{bmatrix} \dot{\hat{i}}_{s\alpha} \\ \dot{\hat{i}}_{s\beta} \\ \dot{\hat{\phi}}_{r\alpha} \\ \dot{\hat{\phi}}_{r\beta} \end{bmatrix} = \begin{bmatrix} -\lambda & \omega_s & \frac{K}{T_r} & K\hat{\omega} \\ -\omega_s & -\lambda & -K\hat{\omega} & \frac{K}{T_r} \\ \frac{L_m}{T_r} & 0 & \frac{1}{T_r} & +\hat{\omega} \\ 0 & \frac{L_m}{T_r} & -\hat{\omega} & \frac{1}{T_r} \end{bmatrix} \begin{bmatrix} \hat{i}_{s\alpha} \\ \hat{i}_{s\beta} \\ \hat{\phi}_{r\alpha} \\ \hat{\phi}_{r\beta} \end{bmatrix} + \begin{bmatrix} \frac{1}{\sigma L_s} & 0 & K & 0 \\ 0 & \frac{1}{\sigma L_s} & 0 & K \\ 0 & 0 & 1 & 0 \\ 0 & 0 & 0 & 1 \end{bmatrix} \begin{bmatrix} v_{s\alpha} \\ v_{s\beta} \\ v_{r\alpha} \\ v_{r\beta} \end{bmatrix} + \begin{bmatrix} L_1 & -L_2 \\ L_2 & L_1 \\ L_3 & -L_4 \\ L_4 & L_3 \end{bmatrix} \times \begin{bmatrix} i_{s\alpha} - \hat{i}_{s\alpha} \\ i_{s\beta} - i_{s\beta} \end{bmatrix} \quad (10)$$

This presentation then takes the following form:

$$\dot{\hat{X}} = A(\omega_r)\hat{X} + BU + L(I_s - \hat{I}_s) \quad (11)$$

with:

$$(I_s - \hat{I}_s) = (i_{s\alpha} - \hat{i}_{s\alpha}, i_{s\beta} - \hat{i}_{s\beta}) = (e_{s\alpha} \quad e_{s\beta})$$

4.3 Speed Estimation by Adaptive Luenberger Observer

Now suppose that the speed is an unknown constant parameter. This involves finding an adaptation law that allows us to estimate it. The state equation of this observer is given by (11)

with:

$$A(\omega) = \begin{bmatrix} -\lambda & \omega_s & \frac{K}{T_r} & \hat{\omega}.K \\ -\omega_s & -\lambda & -\hat{\omega}.K & \frac{K}{T_r} \\ \frac{L_m}{T_r} & 0 & -\frac{1}{T_r} & \hat{\omega} \\ 0 & \frac{L_m}{T_r} & -\hat{\omega} & -\frac{1}{T_r} \end{bmatrix}$$

The speed adaptation mechanism will be deduced from Lyapunov theory, [28], [29], by choosing an adequate candidate function. The estimation error on the stator current and the rotor flux, which is none other than the difference between the observer and the motor model, and given by (5), can be reformulated by:

$$\dot{e} = (A - LC)e + (\Delta A)\hat{X} \quad (12)$$

Or

$$\Delta A = A(\omega) - A(\hat{\omega}) = \begin{bmatrix} 0 & 0 & 0 & K\Delta\omega \\ 0 & 0 & -K\Delta\omega & 0 \\ 0 & 0 & 0 & -\Delta\omega \\ 0 & 0 & \Delta\omega & 0 \end{bmatrix} \quad (13)$$

with:

$$e = (X - \hat{X}) = \begin{pmatrix} e_{is\alpha} & e_{is\beta} & e_{\phi r\alpha} & e_{\phi r\beta} \end{pmatrix}^T$$

and $\Delta\omega = \omega - \hat{\omega}$

Now consider the following Lyapunov function:

$$V = e^T e + \frac{(\Delta\omega)^2}{\lambda} \quad (14)$$

Or λ: Positive constant

The derivative of this function concerning time is:

$$\frac{dV}{dt} = \left\{\frac{d(e^T)}{dt}\right\}..e + e^T.\left\{\frac{de}{dt}\right\} + \frac{2}{\lambda}(\Delta\omega).\frac{d}{dt}(\Delta\omega) \quad (15)$$

We know from (5) that, $\dot{e} = (A - LC)e$, replacing this expression in (15), we obtain:

$$\frac{dV}{dt} = (A - LC)^T e^T.e + e^T(A - LC)e + \frac{2}{\lambda}(\Delta\omega)\frac{d}{dt}\Delta\omega \quad (16)$$

$$\frac{dV}{dt} = e^T\left[(A - LC)^T + (A - LC)\right]e - 2.\Delta\omega.(e_{is\alpha}\hat{\phi}_{r\beta} - e_{is\beta}\hat{\phi}_{r\alpha}) + \frac{2}{\lambda}(\Delta\omega)\frac{d}{dt}\Delta\omega \quad (17)$$

A sufficient condition to have uniform asymptotic stability is that $\frac{dV}{dt} < 0$, which amounts to cancel the last two terms knowing that the first term is negative (imposed by the gain matrix), which implies: $2\Delta\omega.(e_{is\alpha}\hat{\phi}_{r\beta} - e_{is\beta}\hat{\phi}_{r\alpha}) = \frac{2}{\lambda}(\Delta\omega)\frac{d}{dt}\hat{\omega}$, and from this equation, we obtain:

$$\hat{\omega} = \lambda\int_0^t (e_{is\alpha}.\hat{\phi}_{r\beta} - e_{is\beta}.\hat{\phi}_{r\alpha})dt \quad (18)$$

However, this adaptation law is established for a constant speed, and to improve the response of this algorithm, the speed is estimated by a PI regulator, hence the new expression for the speed:

$$\hat{\omega}_r = K_p(e_{is\alpha}\hat{\phi}_{r\beta} - e_{is\beta}\hat{\phi}_{r\alpha}) + K_i\int(e_{is\alpha}\hat{\phi}_{r\beta} - e_{is\beta}\hat{\phi}_{r\alpha}).dt \quad (19)$$

With K_p , and K_i : positive constants.

4.4 Application of Fuzzy Logic to the Leunberger Observer Adaptation Mechanism

In this part, fuzzy control was proposed to improve the performance of sensorless control of DFIM. This method proposes to replace the classic PI speed adaptation mechanism with a fuzzy controller, [30], [31].

4.5 Design of a Fuzzy Adaptation Mechanism of the Luenberger Observer

The input variables of the fuzzy controller are subjected to a defuzzification operation and consequently converted to fuzzy sets. The universe of discourse of each variable of the regulator is subdivided into five fuzzy sets, the latter are represented by membership functions of triangular shape, except for the ends where the trapezoidal shape is used as shown in the Figure 3, [32], [33].

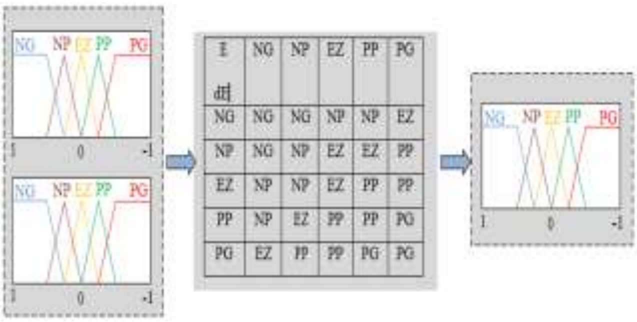

Fig. 3: Internal structure of the Luenberger observer's fuzzy adaptation mechanism

This mechanism takes as input:

- The error E,
- The variation of this error dE,

And outputs the compensation signal u_2.

After processing and integration of the fuzzy inference system, the compensator generates the adequate signal corresponding to its two inputs which are determined by the relation:

$$u_2^*(k) = u_2^*(k-1) + du_2^*(k)$$

The block diagram of the fuzzy Luenberger type observer for estimating the flux and speed is shown in Figure 4.

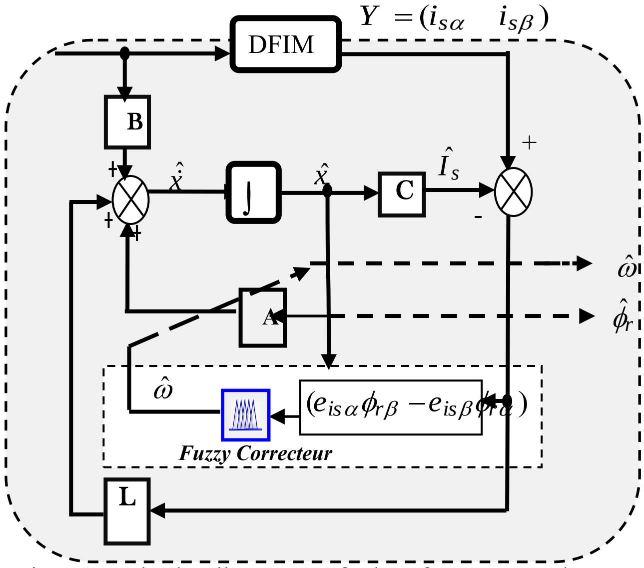

Fig. 4: Block diagram of the fuzzy Luenberger observer

Figure 5 illustrates the general structure of sensorless control of DFIM connected by two 5-level voltage NPC inverters. The rotation speed is estimated by a high gain Luenberger observer improved by fuzzy logic, and the desired speed is compared with a reference, the error of this comparison passes through a PI type regulator to construct the torque reference.

To highlight the performance and robustness of the fuzzy Luenberger observer several cases will be treated, namely, the empty start followed by the introduction of a load torque and the reversal of the direction of rotation, the influence of parametric variations (stator and rotor resistance) on this control. Thus, several dynamic responses will be presented and discussed to validate the control algorithm used. Remember that the speed is regulated by a classic PI and the study is devoted to this one only. The simulation results obtained are represented by the Figure 7 and Figure 8.

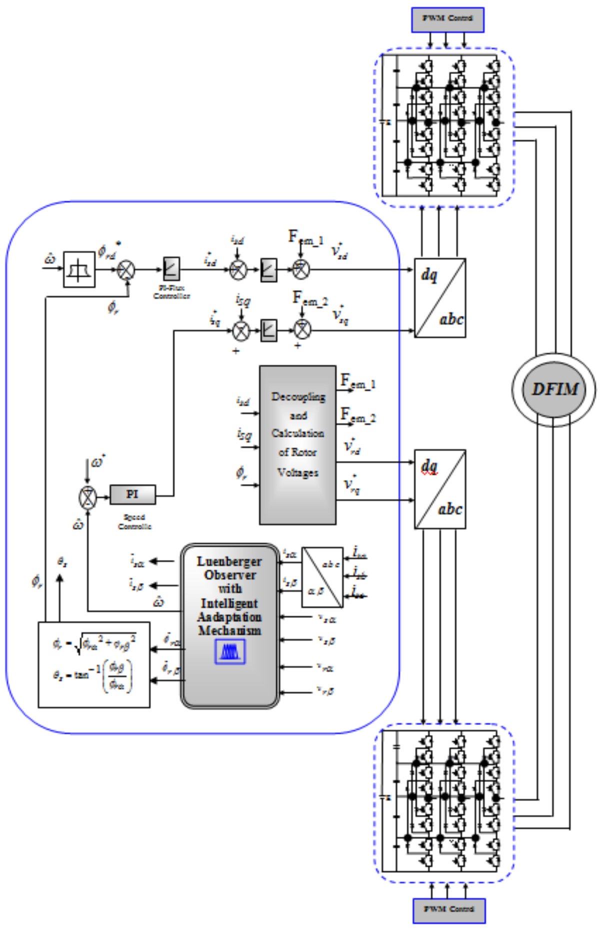

Fig. 5: Global scheme of sensorless direct control by flux orientation of DFIM with intelligent adaptation mechanism of full-order Luenberger observer based on fuzzy logic

5 Simulation Results and Interpretations

To evaluate the performance of the DFIM machine control without a speed and flux sensor, we carried out a series of simulations in a MATLAB/Simulink environment.

The simulations presented in this section are carried out on DFIM powered by a five-level inverter with an NPC voltage structure controlled by PWM, and driven by direct vector control. To carry out this simulation, we took a sampling period of $10^{-3} ms$, the different parameters used are indicated in Table 1:

Table 1. DFIM Parameters

Item	Data
DSIM Mechanical Power	1.5 Kw
Nominal speed	1450 rpm
Pole pairs number	2
Stator resistance	1.68Ω
Rotor resistance	1.75Ω
Stator self-inductance	295 mH
Rotor self-inductance	104 mH
Mutual inductance	165 mH
Moment of inertia	0.01 kg.m^2
friction coefficient	0.0027kg.m^2/s
Nominal Frequency	50 Hz

The simulations are carried out for a simulation time of 3 seconds, and their objectives are:

- Application of a load torque of 10 Nm at time t = 1 sec.
- Elimination of the charge at time t = 2 s.
- Reversal of direction of rotation of time t = 2.5 s.

To be able to test the robustness of the proposed fuzzy Leunberger observer, we applied a parametric variation of the machine up to 50% for the resistances Rr, Rs. The tests carried out are:

- Pursuit test
- A no-load start with a reference scale of 250 rad/s at t=0s
- setpoint change to -250 rad/s at t =2.5s.

Figure 6 shows the simulation results of direct vector control without a velocity and flux sensor with a fuzzy Luenberger observer. We notice an improvement in the overall performance of the system with the insertion of the fuzzy Luenberger observer compared to the PI Luenberger. The curves show that during the empty start, all the quantities stabilize after a response time that lasts 0.2 s, the observed speed is indeed the rotation speed and the reference speed with almost zero static error.

When starting and reversing the direction of rotation, the speed reaches its set value with practically no overshoot. Good rejection of the disturbance due to the application of the load. Decoupling is ensured by this type of observer and regulation. The current is well maintained at its admissible value, and the flux has a very rapid dynamic to reach its reference value. Also, note some additional ripples in torque and current caused by the PWM.

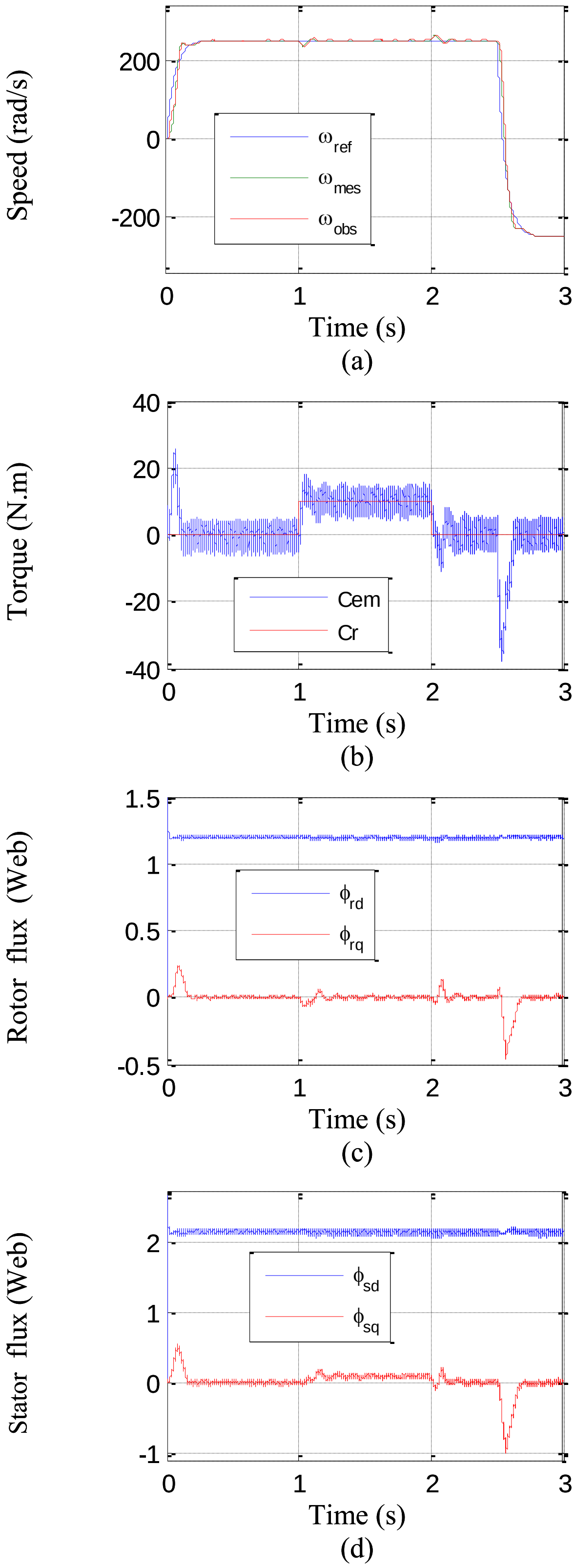

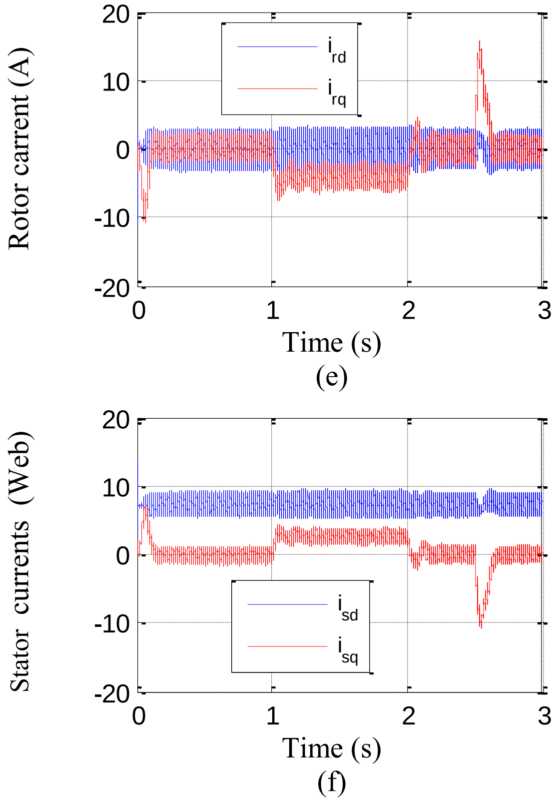

Fig. 6: Simulation results of DFOC without speed sensor based on fuzzy Luenberger observer during an empty start followed by an introduction of a load torque then a reversal of direction of rotation

Figure 7 and Figure 8 present the simulation results of direct vector control with a fuzzy Luenberger observer concerning the variation of the rotor and stator resistance. We note that at each instant of variation of rotor resistance, all the quantities of the machine, namely the speed, the flux, and the electromagnetic torque present a small disturbance especially during the changes in the instructions, and in particular during the reversal of rotation, but this variation in resistance does not degrade the orientation of the flow.

For a nominal value of Rr, the stator resistance Rs is increased by +50% of its nominal value. We also notice that this variation presents a small disturbance during the load application, but it does not degrade the orientation of the flux.

According to the simulation results obtained, we can say that our control without a speed sensor achieves good performance.

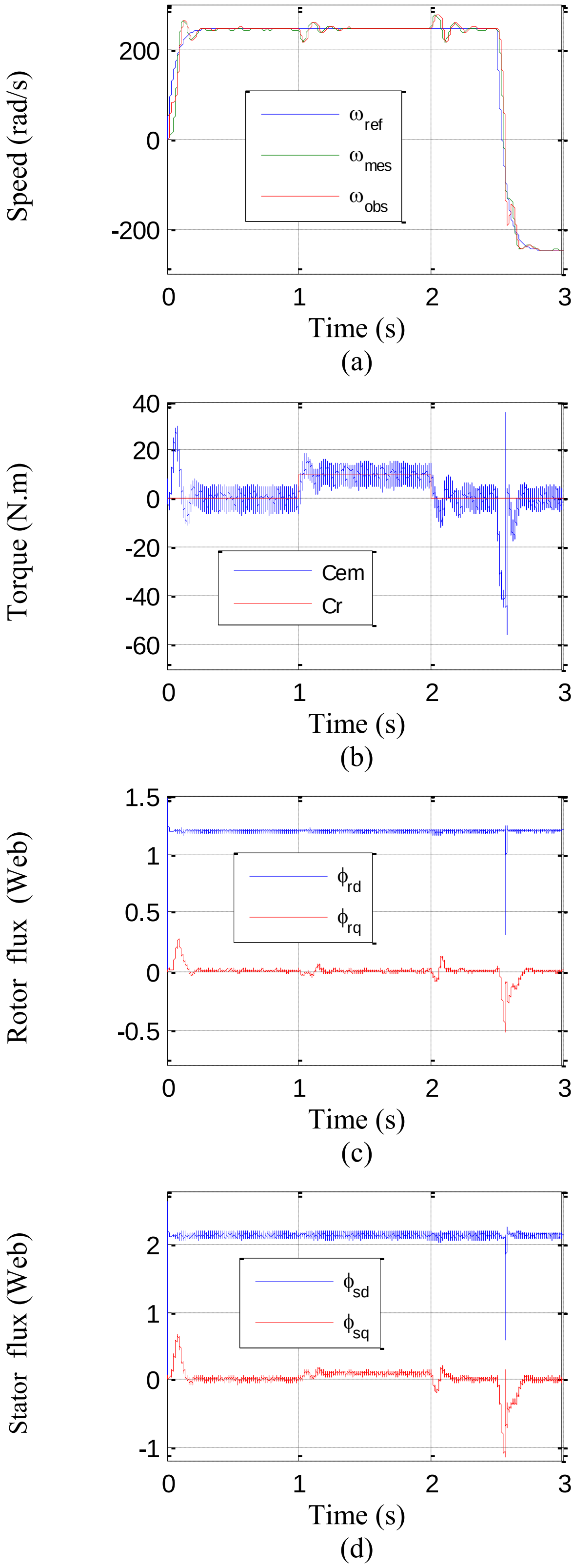

Fig. 7: Simulation results of DFOC without speed sensor based on fuzzy Luenberger observer during variation of +50% of Rr

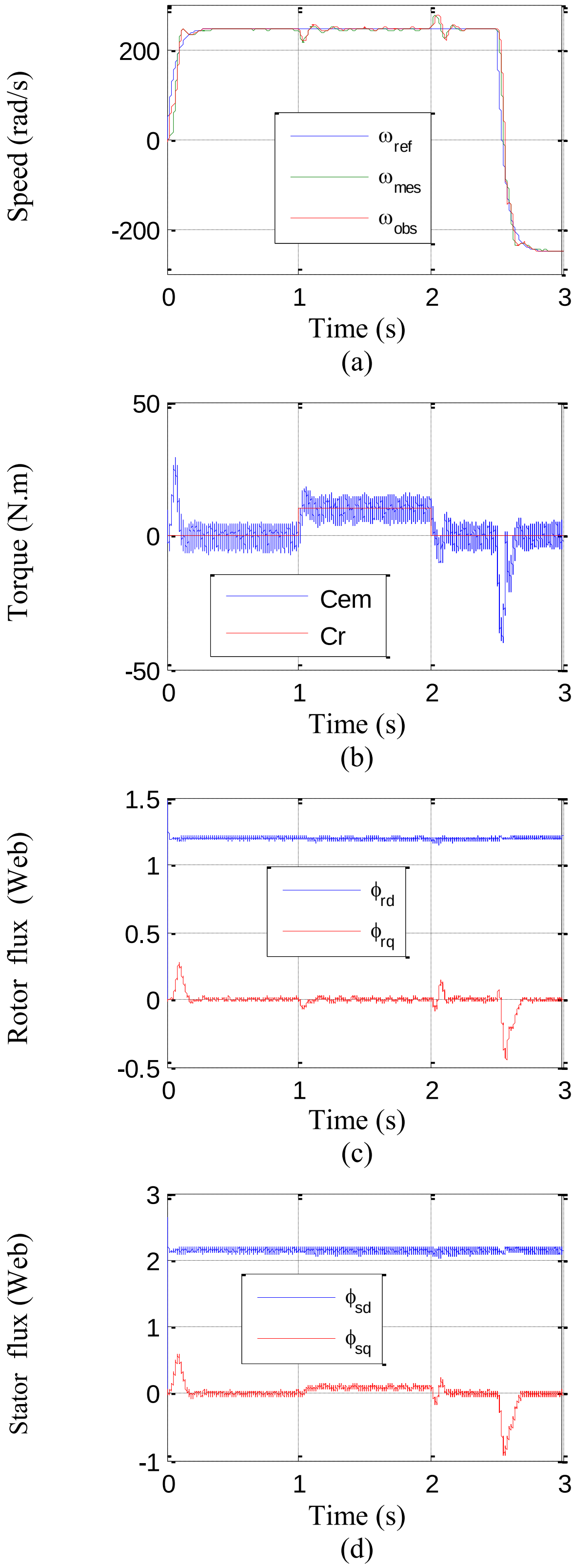

Fig. 8: Simulation results of DFOC without speed sensor based on fuzzy Luenberger observer during variation of +50% of Rs

6 Conclusion

Control without mechanical speed sensors is in full development. It aims to eliminate sensors with their disadvantages such as fragility, cost, and noise.

In this work, we studied the fuzzy Luenberger observer applied to DFIM. This technique is exploited in direct vector control to improve the performance of the sensorless control of the DFIM, powered by two five-level inverters

According to the simulation results obtained, it can be concluded that the proposed estimation technique is valid for nominal conditions, even satisfying basic speed operations, stopping, and even when the machine is loaded. On the other hand, the proposed observer has good robustness concerning the variation of the load and the tracking, making it possible to achieve good functional performances with a low cost and reduced volume installation, this gives a minimal structure to our order.

The work carried out in this paper directs us towards several research perspectives which it seems useful to cite:

1. The application of artificial intelligence regulators instead of traditional regulators to increase the performance of the applied control.
2. Application of other control techniques, such as Backstepping control.

References:

[1] Sudharani, P., Jyotheeswara, R. K. Ritesh, D., Ramakanta, J., Vivekanandan, S., Dhanamjayulu, C. (2022). Direct Torque Control of Induction Motor Using ConvLSTM Based on Gaussian Pillbox Surface. Hindawi. *Mathematical Problems in Engineering*, Article ID 4408271, 21 pages https://doi.org/10.1155/2022/4408271.

[2] Anuchin, A., Bogdanov, A., Demidova, G., Savkin, D., Fedorova, K., Gulyaeva, M. (2020).Model predictive control of a direct current motor utilizing lookup tables. in *Proceedings of the 2020 XI International Conference on Electrical Power Drive Systems (ICEPDS)*, pp. 1–4, Saint Petersburg, Russia, October. https://doi.org/10.1109/ICEPDS47235.2020.9249336.

[3] Wang, Z., Ching, T. W., Huang, S., Wang, H., Xu, T. (2021).Challenges faced by electric vehicle motors and their solutions, *IEEE Access*, vol. 9, pp. 5228–5249. https://doi.org/10.1109/ACCESS.2020.3045716.

[4] Hongxia, Y., Zhicheng, C. (2015). Three-Phase Induction Motor DTC-SVPWM Scheme with Self-tuning PI-Type Fuzzy Controller. *International Journal of Computer and Communication Engineering*, Vol. 4, No.3. https://doi.org/10.17706/IJCCE.2015.4.3.204-210.

[5] Zemmit, A., Messalti, S., Harrag, A. (2018). A new improved DTC of doubly fed induction machine using GA-based PI controller. *Ain Shams Engineering Journal*, Vol. 9, No. 1, pp. 1877–1885. https://doi.org/10.1016/j.asej.2016.10.011

[6] Taoussi, M., Karim, M., Bossoufi, B., Hammoumi, D., Lagrioui, A., Derouich, A (2016). Speed variable adaptive backstepping control of the doubly-fed induction machine drive. *International Journal of Automation and Control*, Vol.10, N°.01, pp. 12-33. https://doi.org/10.1504/IJAAC.2016.075140.

[7] El Ouanjli, N., Derouich, A., El Ghzizal, A. (2019). Direct torque control of doubly fed induction motor using three-level NPC inverter. *Prot Control Mod Power Syst* 4, 17. https://doi.org/10.1186/s41601-019-0131-7.

[8] Djellouli, T,. Moulahoum, S,. Moualdia, A,. Bouchrit, M.S. Wira, P. (2020). Speed Sensorless Direct Torque Control Strategy of a Doubly Fed Induction Motor Using an ANN and an EKF. *Nonlinear Dynamics and Systems Theory*, 20 (4).

[9] Usha, S., Geetha, A., Thamizh, T. M., Thentral, P. V., Tahir, K., Salah, K. (2022). Three Phase Induction Motor Drive: A Systematic Review on Dynamic Modeling, Parameter Estimation, and Control Schemes. *Energies*, 15, 8260. https://doi.org/10.3390/en15218260.

[10] Cherifi, D., Miloud, Y. (2018). Robust Speed-sensorless Vector Control of Doubly Fed Induction Motor Drive Using Sliding Mode Rotor Flux Observer. *International Journal of Applied Power Engineering (IJAPE)*, Vol.7, No.3, pp. 235~250 https://doi.org/10.11591/ijape.v7.i3.pp235-250.

[11] Said, M., Aziz, D., El Ouanjli, N., A Mossa, M., Sagar Bhaskar, M., Ngo, K. L., Nguyen, V. Q. (2022). A New Robust Direct Torque Control Based on a Genetic Algorithm for a Doubly-Fed Induction Motor: Experimental Validation. *Energies*, 15, 5384. https://doi.org/10.3390/en15155384.

[12] Krishna SM, Daya JL, Padmanaban FS, Mihet-Popa L (2017) Real-time analysis of a modified state observer for sensorless induction motor drive used in electric vehicle applications. *Energies* 10(8):1077 https://doi.org/10.3390/en10081077.

[13] Kumar R, Das S, Bhaumik A (2019) Speed sensorless model predictive current control of doubly-fed induction machine drive using model reference adaptive system. *ISA Trans* 86:215–226, https://doi.org/10.1016/j.isatra.2018.10.025.

[14] Korzonek M, Tarchala G, Orlowska-Kowalska T (2019) A review on MRAS-type speed estimators for reliable and efficient induction motor drives. *ISA Trans* 93:1–13, https://doi.org/10.1016/j.isatra.2019.03.022.

[15] Ammar, A., Bourek, A., Benakcha, A. (2019). Robust load angle direct torque control with SVM for sensorless induction motor using sliding mode controller and observer. *Int. J. Computer Aided Engineering and Technology*, Vol. 11, No. 1, pp.14-34, https://doi.org/10.1504/IJCAET.2019.096713.

[16] Ahmed, A. E., Ibrahim, A., Ahmed, M. (2023). Five-level F-type inverter with buck-boost converter-based equalization channels. *Alexandria Engineering Journal* 64, 155–171, https://doi.org/10.1016/j.aej.2022.08.029.

[17] Benamrane, K., Thameur, A., Boualam, B., Bouarroudj, N., Lakhdari, A., Borni, A., Bahri, A. (2022). New Configuration of Five-Level NPC Inverter with Three-Level Boost Converter for Photovoltaic Solar Energy Conversion. *Journal Européen des Systèmes Automatisés*. Vol. 55, No. 4, pp. 519-525, https://doi.org/10.18280/jesa.550411.

[18] Benyoussef, E., Meroufel, A., Barkat, S., (2016). Neural network and fuzzy logic direct torque control of sensorless double star synchronous machine. *Rev. Roum. Sci. Techn. Ectrotechn. et Nerg.* 61(3).

[19] Hassen, R., Saad, B., Ammar, A., Hellali, L. (2019). Enhancement of Space Vector Modulation Based-Direct Torque Control Using Fuzzy PI Controller for Doubly Star Induction Motor. *Advances in Modelling and Analysis C* Vol. 74, No. 2-4, pp. 63-70, https://doi.org/10.18280/ama_c.742-404.

[20] Cherifi, D., Miloud, Y. (2019). Improved Sensorless Control of Doubly Fed Induction Motor Drive Based on Full Order Extended Kalman Filter Observer. *Periodica Polytechnica Electrical Engineering and Computer Science*, pp. 1~10, https://doi.org/10.3311/PPee.14245.

[21] Cherifi, D., Miloud, Y., Mostefai, M. (2021). Performance of Neutral Point Clamped Five Level Inverter Using Space Vector Modulation Control Fed by DPC-VF-SVM Rectifier. WSEAS Transactions on Power Systems, Vol. 16, https://doi.org/10.37394/232016.2021.16.28.

[22] Ronak, A. R., Sujal, A., Anand, M., Chee, W.L., Hee-Je, K. (2019). Review of Multilevel Voltage Source Inverter Topologies and Analysis of Harmonics Distortions in FC-MLI. *Electronics*, 8, 1329, pp: 1-37 https://doi.org/10.3390/electronics8111329.

[23] Kazunori, H., Hirofumi, A. (2011). A new DC-voltage-balancing circuit including a single coupled inductor for a five-level diode-clamped PWM inverter. *IEEE Transactions on Industry Applications*, 47(2), pp. 841-852. https://doi.org/10.1109/TIA.2010.2102327.

[24] Tainton, H., Nkosinathi, G. (2022). Modeling and Vector Control of a Cage+Nested-Loop Rotor Brushless Doubly Fed Induction Motor. *Energies*, 15(14), 5238. https://doi.org/10.3390/en15145238.

[25] Laatra, Y., Aoun, S., Sedraoui, M. (2022). Speed sensorless vector control of doubly fed induction machine using fuzzy logic control equipped with Luenberger observer. *International Journal of Dynamics and Control*, Vol. 10, pages 1876–1888 https://doi.org/10.1007/s40435-022-00946-0.

[26] Karlovský P, Lettl J (2017) Improvement of DTC performance using luenberger observer for flux estimation. *In: 2017 18th international scientific conference on electric power engineering (EPE)*, Kouty nad Desnou, Czech Republic. IEEE, pp 1–5 https://doi.org/10.1109/EPE.2017.7967286.

[27] Holakooie, M.H., Ojaghi, M., Taheri, A. (2016). Full-order Luenberger observer based on fuzzy-logic control for sensorless field-oriented control of a single-sided linear induction motor. *ISA Transactions*, Vol. 60, pp. 96-108, https://doi.org/10.1016/j.isatra.2015.11.022.

[28] Wencen, J., Wang, Y. (2018). An adaptive Luenberger observer for speed-sensorless estimation of induction machines. *Annual American Control Conference*, Milwaukee, USA.

[29] Chaaban, H., Djalaleddine, K., Salim, C. (2020). Sensorless backstepping control using an Luenberger observer for double star

induction motor. *Archives of Electrical Engineering*, 69(1): 101-116.

[30] Tir, Z. (2017). Fuzzy logic field oriented control of double star induction motor drive. *Electrical Engineering*, 99(2): 495-503. https://doi.org/10.1007/s00202-016-0377-2.

[31] Hellali, L., Saad, B. (2018). Speed control of doubly star induction motor (DSIM) using direct field oriented control (DFOC) based on fuzzy logic controller (FLC). *AMSE Journals, Advanced in Modelling and Analysis C,* 73(4): 128-136. https://doi.org/10.18280/ama_c.730402.

[32] Aoun, S., Boukadoum, A., Laatra Y. (2023). Advanced power control of a variable speed wind turbine based on a doubly fed induction generator using field-oriented control with fuzzy and neural controllers. I*nternational Journal of Dynamics and Control* https://doi.org/10.1007/s40435-023-01345-9.

[33] El Ouanjli, N., Taoussi, M., Derouich, A., Chebabhi, A., El Ghzizal, A., Bossoufi, B. (2018). High Performance Direct Torque Control of Doubly Fed Induction Motor using Fuzzy Logic. *Gazi University Journal of Science, GU J Sci* 31(2): 532-542 https://doi.org/10.1186/s41601-019-0131-7.

Contribution of Individual Authors to the Creation of a Scientific Article (Ghostwriting Policy)

The authors equally contributed in the present research, at all stages from the formulation of the problem to the final findings and solution.

Sources of Funding for Research Presented in a Scientific Article or Scientific Article Itself

No funding was received for conducting this study.

Conflict of Interest

The authors have no conflicts of interest to declare.